Therapeutics, Targets, and Chemical Biology

Cancer Research

Novel Mechanistic Insights into Ectodomain Shedding of EGFR Ligands Amphiregulin and TGF-α: Impact on Gastrointestinal Cancers Driven by Secondary Bile Acids

Nagaraj S. Nagathihalli[1,2], Yugandhar Beesetty[1], Wooin Lee[5], M. Kay Washington[3], Xi Chen[4], A. Craig Lockhart[6], and Nipun B. Merchant[1,2]

Abstract

Secondary bile acids (BA) such as deoxycholic acid (DCA) promote the development of several gastrointestinal malignancies, but how they mediate this effect is unclear. In this study, we offer evidence of a mechanism involving ectodomain shedding of the EGFR ligands amphiregulin (AREG) and TGF-α, which rely upon the cell surface protease TACE/ADAM-17. Specifically, we show that AREG participates in DCA-induced EGFR and STAT3 signaling, cell-cycle progression, and tumorigenicity in human colorectal cancer and pancreatic ductal adenocarcinoma (PDAC). TACE and AREG, but not TGF-α, were overexpressed in both colorectal cancer and PDAC tissues compared with normal tissues. Exposure of colorectal cancer and PDAC cells to DCA resulted in colocalization of Src and TACE to the cell membrane, resulting in AREG-dependent activation of EGFR, mitogen-activated protein kinase (MAPK), and STAT3 signaling. Src or TACE inhibition was sufficient to attenuate DCA-induced AREG, but not TGF-α shedding. We also examined a role for the BA transporter TGR5 in DCA-mediated EGFR and STAT3 signaling. RNA interference-mediated silencing of TGR5 or AREG inhibited DCA-induced EGFR, MAPK, and STAT3 signaling, blunted cyclin D1 expression and cell-cycle progression, and attenuated DCA-induced colorectal cancer or PDAC tumorigenicity. Together, our findings define an AREG-dependent signaling pathway that mediates the oncogenic effects of secondary BAs in gastrointestinal cancers, the targeting of which may enhance therapeutic responses in their treatment. *Cancer Res; 74(7); 2062–72. ©2014 AACR.*

Introduction

Dietary intake of a high-fat, low-fiber diet has been associated with increases in secondary bile acids (BA), such as deoxycholic acid (DCA), which is known to activate oncogenic signaling and be promoters of gastrointestinal cancer, including colorectal cancer and pancreatic ductal adenocarcinoma (PDAC; refs. 1–5). Increased production of DCA has also been linked to liver tumorigenesis (6). Most PDACs occur in the head of the gland, which is in close proximity to bile, suggesting that BAs may have a role in the pathogenesis of PDAC (7). Of the BAs implicated in gastrointestinal oncogenesis, DCA is particularly bioactive. However, the mechanism by which DCA promotes tumorigenesis remains to be elucidated.

Authors' Affiliations: Departments of [1]Surgery, [2]Cancer Biology, [3]Pathology, and [4]Biostatistics, Vanderbilt University School of Medicine, Nashville, Tennessee; [5]Department of Pharmaceutical Sciences, University of Kentucky, Lexington, Kentucky; and [6]Department of Medicine, Washington University School of Medicine, St. Louis, Missouri

Note: Supplementary data for this article are available at Cancer Research Online (http://cancerres.aacrjournals.org/).

Corresponding Author: Nipun Merchant, Vanderbilt University, 597 PRB, 2220 Pierce Avenue, Nashville, TN 37232–6860. Phone: 615-322-2391; Fax: 615-343-7622; E-mail: nipun.merchant@vanderbilt.edu

doi: 10.1158/0008-5472.CAN-13-2329

Many G protein-coupled receptor (GPCR) agonists seem to mediate EGFR transactivation by activating EGFR ligand shedding (8, 9). In addition, EGFR is known to activate STAT3 signaling (10). TGR5 is a novel G protein-coupled cell surface BA receptor (11). We have previously shown that DCA-induced signaling is mediated by ligand-dependent phosphorylation of EGFR (12). TGF-α and amphiregulin (AREG), two ligands that bind to the EGFR and are upregulated frequently in colorectal cancer (13). Proteolytic processing of these ligands requires TNF-α converting enzyme/a disintegrin and metalloprotease-17 (TACE/ADAM-17; refs. 13, 14). TACE plays a key role in EGFR signaling and has recently emerged as a potential therapeutic target in several tumor types (15). In polarized epithelial cells, EGFR is restricted predominantly to the basolateral surface. TGF-α and AREG are delivered selectively to this compartment in which they are both cleaved by TACE to release mature, soluble ligands that then bind to the receptor (13, 16). We have shown that TACE is upregulated in colorectal cancer and is a viable target of the EGFR axis in colorectal cancer (13). TACE also plays a critical role in the cellular crosstalk (transactivation) between GPCR and EGFR signaling (17, 18). In head and neck cancer, GPCR activation of TACE and subsequent shedding of AREG is mediated by c-Src (Src; refs. 17, 18). Src is frequently overexpressed in colorectal cancers and PDACs (19, 20) and its expression and activity correlates with cancer progression, advanced malignancy, and poor prognosis in a variety of human cancers (20–23).

Previous studies have provided evidence for a role of Src family kinases in the activation of TACE (18, 24, 25). Whether the TGR5 receptor mediates DCA-induced activation of cellular signaling to regulate tumorigenicity is not known. We have also shown that increased membranous Src expression results in decreased survival in patients with PDAC (20).

Therefore, we hypothesized that Src may interact with TACE to mediate AREG and TGF-α ligand cleavage. Our results show that DCA stimulates Src and TACE association and colocalization to the cell membrane, which results primarily in shedding of AREG to activate EGFR, MAPK (mitogen-activated protein kinase), and STAT3 signaling and induce tumorigenicity of both PDAC and colorectal cancer. We further show that DCA-induced activation of cellular signaling is mediated by the TGR5 GPCR. These results support EGFR ligands as valid targets for human colorectal cancer and PDAC therapy. In the era of kinase inhibitors, this study supports the significance of AREG and TACE inhibition as an effective strategy in the treatment of colorectal cancer and PDAC.

Materials and Methods

Cell lines and gene knockdown analysis

Human colorectal cancer cell lines HCT-116 and HCA-7 (generous gift from Dr. Susan Kirkland, Royal Postgraduate Medical School, London, England; *Mycoplasma*-negative tested by a PCR detection method using the Sigma Venor-Gem Kit), PDAC cell lines BxPC-3, AsPC-1, and Capan-2 were obtained from the American Type Culture Collection (ATCC) and were maintained according to their specifications. ATCC cell lines were characterized and were free of *Mycoplasma* contamination, tested by Hoechst DNA stain (indirect) and agar culture (direct) methods.

Open biosystems pGIPZ–based short hairpin RNA (shRNA) lentiviral vectors were used to deplete Src or TACE expression. Lentiviral shRNA vector pGIPZ with either targeting sequences for knocking down human Src (clone IDs, V2LHS_262793 and V2LHS_70230) and TACE/ADAM17 (clone ID, V2LHS_153732) or nonsilencing control sequence was obtained from Vanderbilt University Microarray Core. Transfection was performed using FuGENE 6 transfection reagent (Roche) following the manufacturer's instructions. Details provided in Supplementary Materials and Methods.

SMARTpool siRNA to target human AREG (M-017435; GenBank accession no. NM_001657), TGF-α (L-019737; GenBank accession no. NM_003236), and TGR5 (J-005519; GenBank accession no. NM_001077194) was purchased from Dharmacon. Transfection of siRNA was performed using DharmaFECT siRNA transfection reagent. Nontargeting control siRNA (Dharmacon; D-001810) and GAPDH (glyceraldehyde-3-phosphate dehydrogenase) control siRNA (Dharmacon, D-001830) were used as negative and positive controls, respectively.

Pancreas tissue microarray

Pancreas tissue microarrays (TMA) were constructed as previously described (26). The patient demographics characteristics were as previously described (20). TMA slides were concurrently evaluated by two of the authors (M.K. Washington and N.B. Merchant). Staining was scored as follows: the staining index was considered as the sum of the intensity score (0, no staining; 1+, weak; 2+, moderate; and 3+, strong) and the distribution score (0, no staining; 1+, staining of <33% of cells; 2+, between 33% and 66% of cells; and 3+, staining of >66% of cells). TACE, AREG, and TGF-α expression was scored as positive if any detectable membranous or cytoplasmic staining was present. The χ^2 test was used to examine the independence of scores with normal and tumor status.

Radioimmunoassay for AREG and TGF-α

We have developed a highly specific and reproducible solid-phase radioimmunoassay for accurate measurements of human AREG and TGF-α in the medium as well as in cell lysates (12, 27). On the basis of dose-escalation experiments, a dose of 300 μmol/L was identified as the optimal dose at which DCA stimulates AREG and TGF-α release with minimal cell death.

Immunoprecipitation and Western blot analysis

Immunoprecipitation and Western blot analysis were performed as previously described (20). Cells were grown in complete media overnight and then treated with DCA as required with or without WAY-022 (1 μmol/L) or PP2 (2 μmol/L) or erlotinib (100 nmol/L) in each assay. For immunoprecipitation, protein lysate was incubated with TACE/ADAM17 polyclonal antibody for 2 hours at 4°C, followed by incubation with 20 μL of protein G-sepharose beads (Sigma) for 1 hour. The immune complexes were analyzed. The input lanes are loaded with 5% of protein lysate used for immunoprecipitation and immunoblotted for β-actin. Relative blot intensities were quantitated by using the NIH ImageJ software.

Immunofluorescence assay

Cells were grown and treated with DCA (300 μmol/L) for 6 hours, fixed, and stained with anti-TACE or anti-Src as previously described (20).

TACE activity assay

TACE activity was measured using the InnoZyme TACE Activity Kit (Calbiochem). Cells were treated, lysed, and were subjected to the TACE activity assay following the manufacturer's instructions.

RNA isolation and quantitative reverse transcription PCR analyses

RNA isolation and quantitative reverse transcription (RT)-PCR analyses were performed as described before (28). Primary sequences are shown in Supplementary Table S1.

Luciferase assays

Cyclin D1–Luc (29) was used to study the promoter activity. The luciferase activity was determined using a dual-luciferase reporter assay kit (Promega). The relative luciferase activity was determined after 48 hours of transfection and normalized to protein concentration.

Cell-cycle analysis

Cells were harvested, stained, washed, and resuspended as described before (20, 30). Cell fluorescence signals were

determined using a FACSCaliber flow cytometer and analyzed with its Cell Quest software.

Cell invasion assay

Cells were seeded into the upper chamber of 8-μmol/L pore Transwell coated with 50 μL (~100 μg) of diluted Matrigel (BD Biosciences) solution and invasion assay was performed as previously described (31).

Cell proliferation assay (WST-1)

Cell proliferation assay was done using a premix WST-1 cell proliferation assay system (Roche Applied Science) following the manufacturer's instructions. Cells were seeded on 96-well plates at a density of 2×10^3 per well in 100 μL culture medium. Cells were incubated for 1 to 4 days and subsequently exposed to 10 μL WST-1 reagent for 2 hours. The absorbance was measured at 450 nm as the detection wavelength and 670 nm as the reference wavelength for the assay.

Statistical analysis

Results are shown as values of mean ± SD unless otherwise indicated. Statistical analyses were performed using the ANOVA followed by the Tukey multiple comparisons test to determine *P* values unless otherwise indicated.

Results

DCA induces Src and TACE colocalization to the cell membrane

To elucidate the mechanism involved in regulating the interaction between Src and TACE, we examined the effect of the tumor-promoting secondary BA DCA on TACE and Src association by immunoprecipitation in human colorectal cancer lines HCT-116, HCA-7, as well as the human PDAC cell line BxPC-3. In all cell lines studied, DCA exposure increased the association of Src with TACE (Fig. 1A). By immunofluorescence imaging, in the absence of DCA, TACE, and Src are present mainly in the cytoplasm, whereas treatment with DCA induced a coordinate redistribution of both Src and TACE to the cell membrane (Fig. 1B). These results show that DCA induces association of Src and TACE, in conjunction with their translocation to the cell membrane.

Src and TACE are required for DCA-induced AREG and TGF-α shedding

Our previous observations confirm a role for TACE in the constitutive shedding of AREG and TGF-α and activation of EGFR signaling (13). To further define the roles of TGF-α and AREG in DCA-induced EGFR activation, we evaluated the effects of DCA on these ligands. TGF-α mRNA levels peaked at 4 hours of incubation with DCA and then declined, whereas AREG mRNA levels continually increased up to 24 hours after DCA exposure (Supplementary Figs. S1A and S1B).

We next examined the effect of silencing Src or TACE on DCA-induced TGF-α and AREG shedding and cellular expression. Interestingly, the knockdown of TACE, but not Src, showed a significant decrease in the mRNA expression of AREG and TGF-α (Supplementary Figs. S1C and S1D). In empty

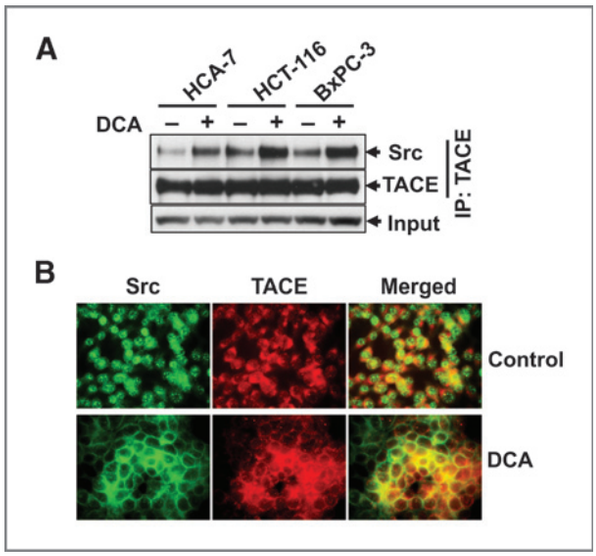

Figure 1. Src associates with TACE in DCA-treated colorectal cancer and PDAC cells. A, cells were treated with DCA (300 μmol/L) for 6 hours, followed by immunoprecipitation (IP) with TACE and immunoblotted for Src. The membrane was stripped to immunoblot for TACE to ensure equal loading. As an input control before immunoprecipitation, an immunoblot with whole-cell lysate was stained for β-actin. B, HCT-116 cells were treated with DCA (300 μmol/L) for 6 hours, double stained with anti-TACE (red) and anti-Src (green) antibody.

vector cells, DCA exposure dramatically increased shedding of both ligands into the media (Fig. 2A) as well as expression levels of ligands in the cell lysates (Supplementary Figs. S2A and S2B) in a time-dependent manner. In HCT-116 shRNA Src or TACE cells, the extent of DCA-induced AREG and TGF-α shedding and their expression in cell lysates was significantly lower compared with the vector controls (Figs. 2A and Supplementary Fig. S2A). The decrease in shedding and lysate expression was more dramatic and sustained for AREG compared with TGF-α, which although inhibited, continued to increase over time in both Src and TACE shRNA cells. Similar results were seen in PDAC BxPC-3 cells—shRNA-mediated silencing of Src or treatment with the TACE inhibitor WAY-022 resulted in significant inhibition of AREG shedding (Fig. 2B and C) and cell lysate expression (Supplementary Fig. S2B), whereas TGF-α shedding was not affected. AREG shedding was also increased in PDAC (AsPC-1 and Capan-2) cells exposed to DCA (Supplementary Fig. S2C). These results confirm the importance of both Src and TACE in DCA-induced sheddase activity and further indicate that DCA primarily stimulates shedding of AREG and not TGF-α through this Src-TACE–mediated pathway.

Src is required for DCA-induced TACE-mediated EGFR phosphorylation

DCA exposure stimulates phosphorylation of Src in HCT-116, BxPC-3, and capan-2 cells (Fig. 3A). Following our previous observations, we sought to determine whether the cell surface activation of TACE is regulated by DCA-induced Src phosphorylation. DCA-induced phosphorylation of TACE was

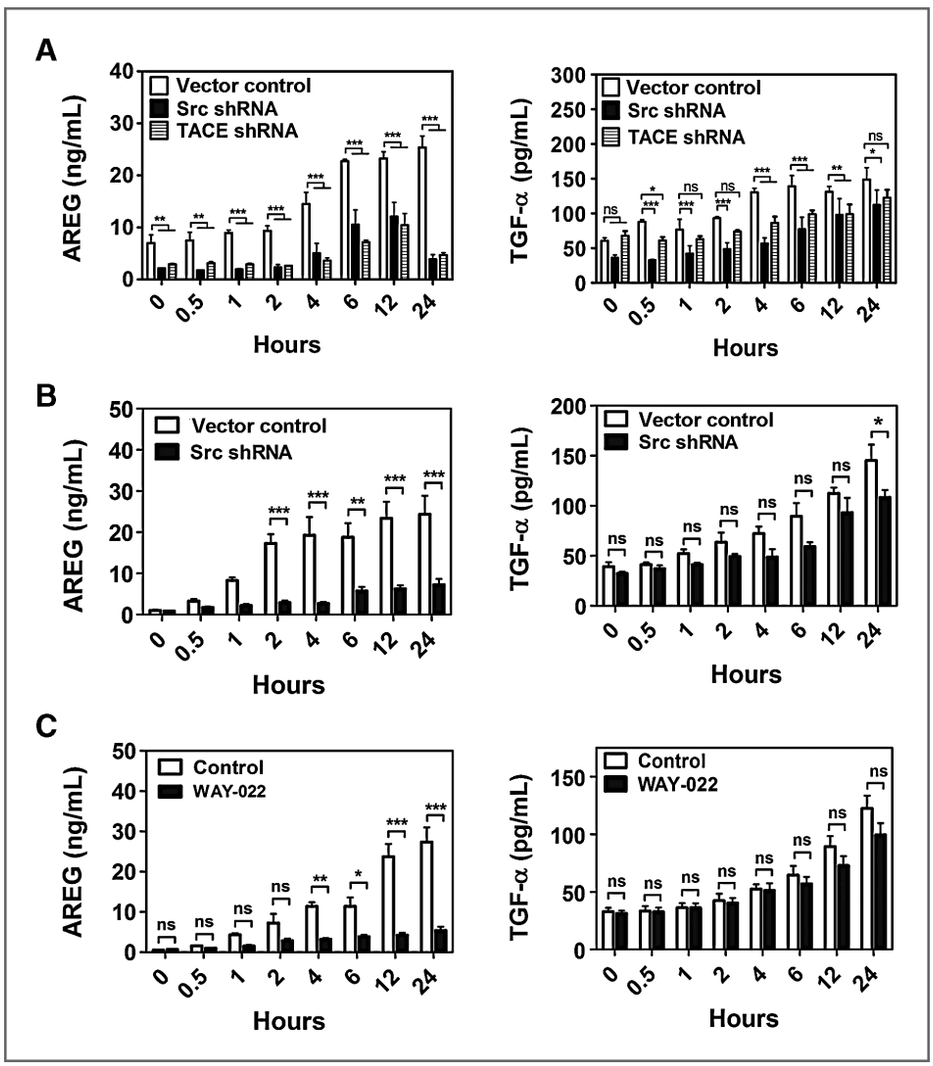

Figure 2. Src and TACE association mediates DCA-induced AREG and TGF-α shedding. Cells were treated with DCA (300 μmol/L) for up to 24 hours. Media were collected for radioimmunoassay analysis of AREG and TGF-α from stably expressing Src and TACE shRNA of HCT-116 cells (A), and Src shRNA (B) and WAY-022 (1 μmol/L; C)–treated BxPC-3 cells and analyzed as described in Materials and Methods. AREG and TGF-α secretion are indicated as ng/mL and pg/mL, respectively. Individual data point, mean ± SD ($n = 3$; *, $P < 0.05$; **, $P < 0.01$; ***, $P < 0.001$; ns, nonsignificant).

abrogated by the Src inhibitor PP2 in both HCT-116 and BxPC-3 cells (Fig. 3B). Furthermore, the extent of DCA-induced TACE and EGFR phosphorylation was significantly inhibited in Src shRNA HCT-116 (Fig. 3C) and BxPC3 (Supplementary Fig. S3A) cells compared with vector control cells.

Similarly, we observed a significant decrease in DCA-induced EGFR phosphorylation in TACE shRNA cells compared with the vector control cells, which retained the ability to phosphorylate both TACE and EGFR (Fig. 3C). Consistent with these results, TACE sheddase activity in DCA-treated cells was significantly enhanced (Fig. 3D). Both Src and TACE shRNA (Fig. 3D), as well as pharmacologic inhibition of Src and TACE with PP2 and WAY-022 (Fig. 3E), respectively, resulted in a significant decrease of DCA-induced TACE activity and phosphorylation of EGFR (Fig. 3F) in HCT-116 and BxPC-3 cells. Collectively, these results show that DCA-induced phosphorylation of TACE is Src-dependent, whereas EGFR activation is dependent on phosphorylation of both Src and TACE in both colorectal cancer and PDAC cells.

AREG is a critical ligand responsible for DCA-induced EGFR and STAT3 signaling

Our findings show that TACE and AREG may be the more important protease/ligand pair for DCA-induced EGFR activation in both colorectal cancer and PDAC. We detected a robust immunoreactive AREG band in DCA-treated cells compared with untreated HCT-116, HCA-7, BxPC-3, and capan-2 cells (Fig. 4A). Both TACE inhibition with WAY-022 and Src inhibition with PP2 significantly inhibited AREG shedding into the conditioned medium in both HCT-116 and BxPC-3 cells (Supplementary Fig. S3B). These results show that Src mediates DCA-induced AREG shedding in these cells. TGF-α, however, does not seem to be a critical ligand responsible for DCA-induced EGFR signaling (Supplementary Results and Supplementary Fig. S4). In additional experiments, we show that MAPK inhibition with U0126 attenuates DCA-induced cell-cycle synthesis (Supplementary Fig. S4C) and proliferation (Supplementary Fig. S4D), showing that DCA-induced proliferation is MAPK mediated.

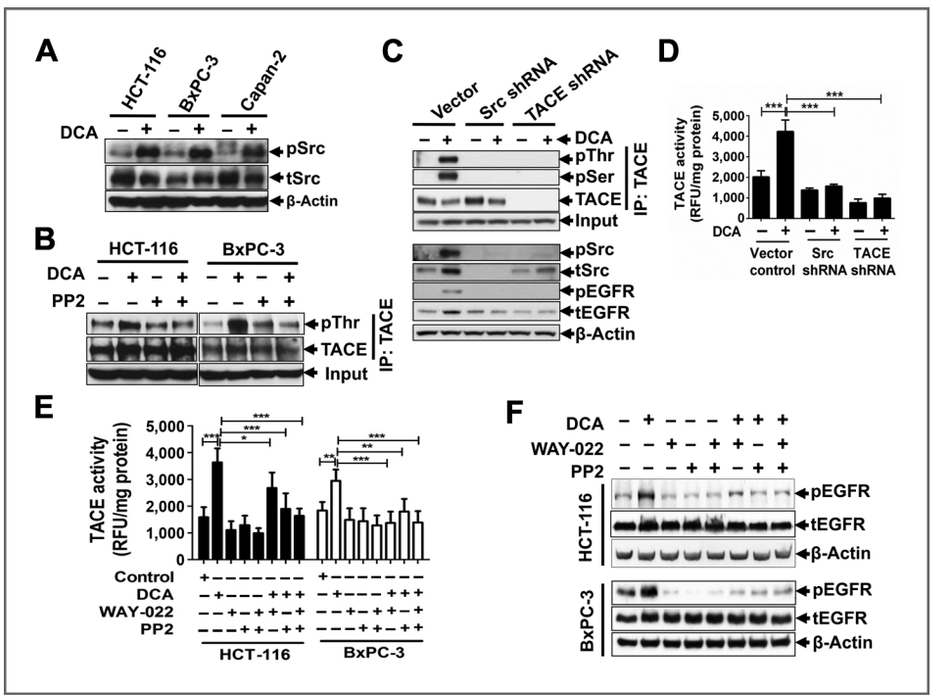

Figure 3. Src and TACE association mediates EGFR signaling. A, cells were treated with DCA (300 μmol/L), lysed, and analyzed by immunoblot to determine the phosphorylation status of Src. B, cells were treated with DCA with or without PP2 (5 μmol/L) and then subjected to TACE immunoprecipitation (IP) followed by phospho-threonine and TACE immunoblot. C, HCT-116 Src shRNA and TACE shRNA cells and vector control cells were treated with DCA for 12 hours, lysed, and analyzed by immunoblot to determine the phosphorylation status of Src, TACE and EGFR. Cell lysates were subjected to TACE immunoprecipitation followed by immunoblot analysis for phosphorylation of threonine and serine. As an input control before immunoprecipitation, an immunoblot analysis with whole-cell lysate was stained for β-actin. Immunoblot analysis data are from at least two representative studies with similar results. D, HCT-116 Src shRNA and TACE shRNA cells and vector control cells were treated with DCA for 12 hours. TACE activity in the cell lysates was measured. Fluorescence intensity was measured and displayed in relative fluorescence units (RFU) per milligram of protein. E and F, cells were treated with Src kinase inhibitor PP2 (5 μmol/L) and/or TACE inhibitor WAY-022 (1 μmol/L) for 1 hour before treating with DCA for 12 hours. E, TACE activity in the cell lysates was measured. D and E, individual data point, mean ± SD ($n = 3$; *, $P < 0.05$; **, $P < 0.01$; ***, $P < 0.001$). F, cells were lysed and analyzed by immunoblot to determine the phosphorylation status of EGFR.

Next, we investigated AREG regulation in DCA-mediated EGFR and STAT3 signaling. AREG siRNA cells showed decreased AREG protein expression in HCT-116, HCA-7, capan-2, and BxPC-3 cells (Supplementary Fig. S5A and S5B). DCA exposure led to increased expression of phosphorylated MAPK in a concentration-dependent manner (Supplementary Fig. S5C). However, although DCA exposure at 10 μmol/L resulted in an increase in STAT3 phosphorylation, higher concentrations of DCA resulted in attenuation of STAT3 phosphorylation (Supplementary Figs. S5D and S8C). To further confirm the importance of AREG in DCA-induced EGFR, MAPK, and STAT3 signaling, we show that AREG siRNA HCT-116 and BxPC3 cells resulted in significant attenuation of DCA-induced EGFR and MAPK phosphorylation (Fig. 4B and C), STAT3 phosphorylation (Fig. 4D), as well as cyclin D1 expression compared with scrambled control cells (Fig. 4B). These results further substantiate the importance of AREG as a critical ligand in BA-mediated EGFR and STAT3 signaling.

AREG is responsible for DCA-induced cyclin D1 promoter activity and cell-cycle regulation

DCA exposure stimulates upregulation of cyclin D1 mRNA expression (Fig. 5A and B) and promoter activity (Fig. 5C). In AREG siRNA cells, there was a significant attenuation of DCA-induced cyclin D1 expression ($P < 0.001$; Fig. 5B) and promoter activity ($P < 0.01$; Fig. 5C) as well as a decrease in the percentage of cells in S-phase (Fig. 5D). Cells treated with DCA showed an increase in DNA synthesis and cell proliferation rate in vector control cells as determined by [^{3}H] thymidine incorporation assay (Supplementary Fig. S6A), whereas Src shRNA cells or EGFR inhibition with erlotinib showed significant inhibition of DNA synthesis rate (Supplementary Fig. S6B) as well as a significant decrease in cyclin D1 promoter activity (Supplementary Fig. S6C). These results indicate that Src-mediated AREG shedding is involved in DNA synthesis and cyclin D1 promoter activity. Moreover, targeting AREG decreased DCA-induced cell proliferation, colony formation, migration, and invasion (Supplementary Fig. S7). This confirms the importance of AREG as a critical ligand in the regulation of DCA-induced EGFR-dependent tumorigenicity.

TGR5, a BA receptor responsible for DCA-induced signaling

TGR5 interacts with a broad range of BAs, including DCA (32). We first sought to determine the presence of the TGR5 receptor in BxPC-3 and HCT-116 cells. RT-PCR results showed

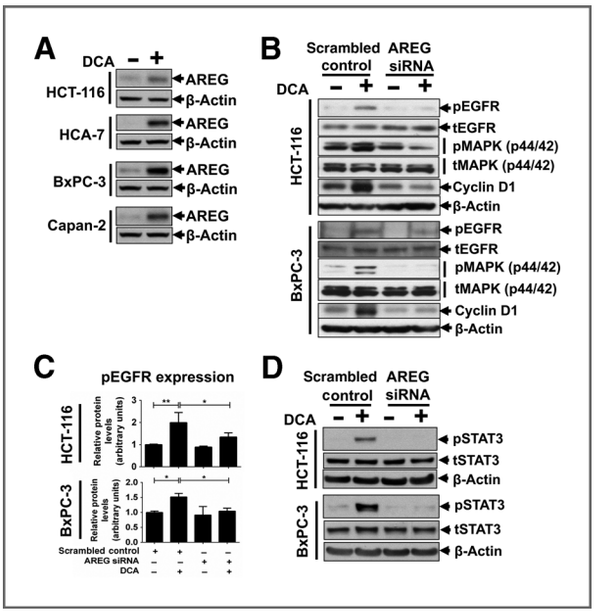

Figure 4. AREG is responsible for DCA-induced EGFR and STAT3 signaling. A, cells were treated with DCA for 12 hours, lysed, and analyzed for AREG by immunoblot. B, HCT-116 and BxPC-3 AREG siRNA cells were treated with DCA for 12 hours, lysed, and investigated further by immunoblot analysis for phosphorylation of EGFR and MAPK and expression of cyclin D1. Immunoblot analysis data are from at least three representative studies with similar results. C, quantitative analysis from three independent immunoblots of EGFR phosphorylation normalized to total EGFR expression levels (mean ± SD; $n = 3$; *, $P < 0.05$; **, $P < 0.01$). D, HCT-116 and BxPC-3 AREG siRNA cells were treated with DCA (10 μmol/L), lysed, and analyzed by immunoblot to determine the phosphorylation status of STAT3.

that TGR5 mRNA was present in BxPC-3 when compared with FLO (esophageal adenocarcinoma) cells, which are known to express TGR5 (Supplementary Fig. S8A; ref. 33). To determine whether TGR5 is involved in DCA-induced activation of Src, EGFR, and STAT3 signaling, TGR5-specific siRNA was transfected into BxPC-3 cells (Supplementary Fig. S8B). In TGR5 siRNA BxPC-3 cells, DCA exposure resulted in significantly attenuated phosphorylation of Src, EGFR, MAPK, STAT3, and cyclin D1 expression compared with TGR5 scrambled control BxPC3 cells (Fig. 6A), showing that TGR5 receptor contributes to DCA-induced activation of Src, EGFR, and STAT3 signaling. Furthermore, BxPC3 TGR5 siRNA cells also showed a decrease in the expression of AREG (Fig. 6B), suggesting the involvement of TGR5 in the DCA-induced AREG expression.

TGR5 is involved in the DCA-induced EGFR-mediated cyclin D1 regulation, cell invasion, and cell proliferation

EGFR activity has been shown to be required for GPCR-induced cell-cycle progression by increasing the level of cyclin D1 (34). Therefore, we assessed whether TGR5 is involved in DCA-induced cyclin D1 regulation. Our results show that DCA induced cyclin D1 protein expression (Fig. 4B) and mRNA expression levels (Fig. 5A) in different colorectal cancer and PDAC cell lines. However, BxPC3 TGR5 siRNA cells showed a significant decrease in cyclin D1 mRNA expression (Fig. 6C) as well as a decrease in cyclin D1 promoter activity (Fig. 6D), suggesting the involvement of TGR5 in the DCA-induced cell-cycle regulation. Compared with scrambled control cells, silencing TGR5 did not affect phosphorylation of STAT3 (Fig. 6E) and cell invasion (Fig. 6F). However, DCA-induced STAT3 activation (Fig. 6E), cell invasion (Fig. 6F), and proliferation (Fig. 6G) were significantly inhibited in TGR5 siRNA cells. These results confirm that TGR5 is involved in DCA-induced cell invasion and proliferation of human cancer cells.

The combination of EGFR inhibition using erlotinib TGR5 siRNA cells, however, did not show a significant difference in DCA-induced phosphorylation of STAT3 (Supplementary Fig. S8C) cell proliferation (Supplementary Fig. S8D) compared with either erlotinib treatment or TGR5 silencing alone (Supplementary Results). These results further substantiate the importance of TGR5-dependent EGFR transactivation and cyclin D1 activity to stimulate cell proliferation and invasion.

TACE, AREG, and TGF-α expression in human pancreas tissues

We have previously shown that TACE and AREG, but not TGF-α, are overexpressed in human colorectal cancer tissue compared with the normal colonic mucosa (13). We, therefore, sought to determine the expression of TGF-α, AREG, and TACE in human pancreatic tissue. Figure 7A depicts the distribution of difference in intensity staining score between normal ducts and PDACs for TACE, AREG, and TGF-α. The staining indices of TACE, AREG, and TGF-α varied significantly between normal pancreas and PDAC tissues. Analysis confirmed a significant increase in the expression of TACE and AREG in PDAC tumor tissue compared with normal pancreas (Fig. 7B). The average intensity of staining of both TACE and AREG was significantly higher in PDAC tumors compared with normal pancreas ($P = 0.045$ and 0.009, respectively). On the other hand, there was no difference in staining intensity of TGF-α between normal pancreas tissue and PDACs ($P = 0.485$). These results indicate that TACE and AREG expression increases with the progression of pancreatic neoplasia, further supporting the importance of AREG as the primary ligand involved in colorectal cancer and PDAC cancer progression.

Discussion

BAs promote tumorigenesis by stimulating a variety of mitogenic receptor tyrosine kinase signaling pathways (35). The molecular mechanisms of the tumor-promoting actions of secondary BAs remain poorly understood. BAs have been shown to transactivate EGFR signaling (36). EGFR inhibitors in solid tumors have shown only modest clinical responses, suggesting the need to implement combination therapies with novel targeted molecules to improve efficacy (37, 38). To this end, understanding the upstream cascade that leads to EGFR activation is essential to determine the mechanism underlying its oncogenic potential and chemoresistance.

Previously, we showed that TACE is restricted to the basolateral surface of the plasma membrane of polarizing colorectal cancer cells and demonstrated that TACE and

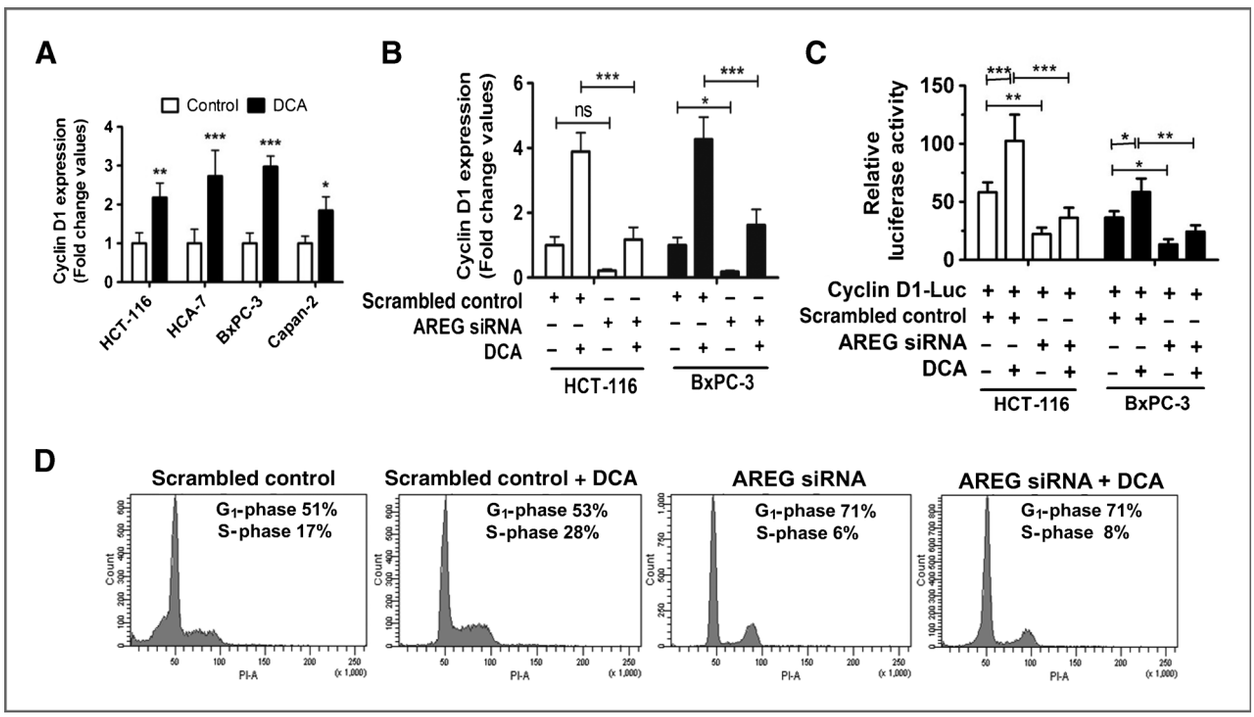

Figure 5. AREG is responsible for DCA-induced cell-cycle regulation. A and B, cells were treated with DCA (300 μmol/L) for up to 24 hours and assessed for transcription of the cyclin D1 gene using quantitative real-time PCR. C, the luciferase assay using the cyclin D1 reporter for cyclin D1 transcriptional activity with DCA exposure in scrambled control cells and AREG siRNA cells. B and C, individual data point, mean ± SD ($n = 3$; *, $P < 0.05$; **, $P < 0.01$; ***, $P < 0.001$). D, cell-cycle analysis of BxPC-3 scrambled control cells, AREG siRNA BxPC-3 cells were conducted with DCA exposure.

AREG are overexpressed in primary and metastatic colorectal cancer compared with normal colonic mucosa (13). Here, we show that the association of Src and TACE at the cell membrane mediates ectodomain shedding of EGFR ligands and is an important mechanism of EGFR transactivation. Furthermore, TACE mediates ligand shedding in response to DCA-induced Src activation. In both colorectal cancer and PDAC cells, DCA primarily stimulates shedding of AREG and not TGF-α. Ectodomain shedding of AREG comprises an important regulatory mechanism because it generates a functional soluble molecule through multiple mechanisms, to provide important proliferative and survival advantages (39, 40). Our results indicate a pivotal role of DCA-induced AREG proligand cleavage leading to activation of EGFR signaling and tumorigenicity.

We show that TGR5, a GPCR is present in BxPC-3 and HCT-116 and mediates DCA-induced activation of EGFR and STAT3 signaling through AREG (Fig. 6). These results are consistent with the previous finding that GPCR activation induce AREG-dependent EGFR signaling in squamous cell carcinoma of the head and neck (HNSCC; ref. 17) and also consistent with our previous reports showing autocrine secretion of AREG by premalignant and malignant colorectal cancer cells (41). We and others have shown increased AREG expression in colorectal cancer tumors (13, 42), and we now show that both TACE and AREG are also overexpressed in PDAC tumors (Fig. 7). Therefore, it is plausible that AREG is indispensable for malignant transformation of colorectal cancer and PDAC.

Translocation of Src and TACE to the plasma membrane likely plays an important role in TACE function by placing TACE in the proximity of its pro-ligand targets. Moreover, we have previously shown that patients with PDAC that have increased membranous Src expression have a significantly lower overall survival than in patients with tumors that have higher cytoplasmic expression of Src (20). The mechanism by which Src associates with TACE following DCA treatment could involve the proline-rich sequence in the cytoplasmic domain of TACE and the Src homology 3 domain of Src. The p85 protein has been shown to interact with both TACE and Src (18) and may be acting as an intermediary between the two molecules. Several observations suggest that the interaction between TACE and Src is of physiologic significance and activated forms of Src can stimulate the EGFR and ERK signaling by activation of TACE and release of EGFR ligands (24). First, the transactivation of EGFR and the activation of downstream MAPK, in response to DCA, require active Src. Second, stimulation of these cancer cells with DCA results in increased TACE and Src association. Third, TACE translocates with Src to the plasma membrane in which TACE-induced cleavage of AREG occurs. Finally, DCA stimulation of PDAC and colorectal cancer cells induce TACE phosphorylation in a Src-dependent fashion.

Knockdown of AREG expression results in substantial attenuation of basal EGFR, MAPK, and STAT3 phosphorylation, key signaling pathways in most human cancers (43, 44). A similar role for AREG in the transactivation of the EGFR in HNSCC has also been reported (17).

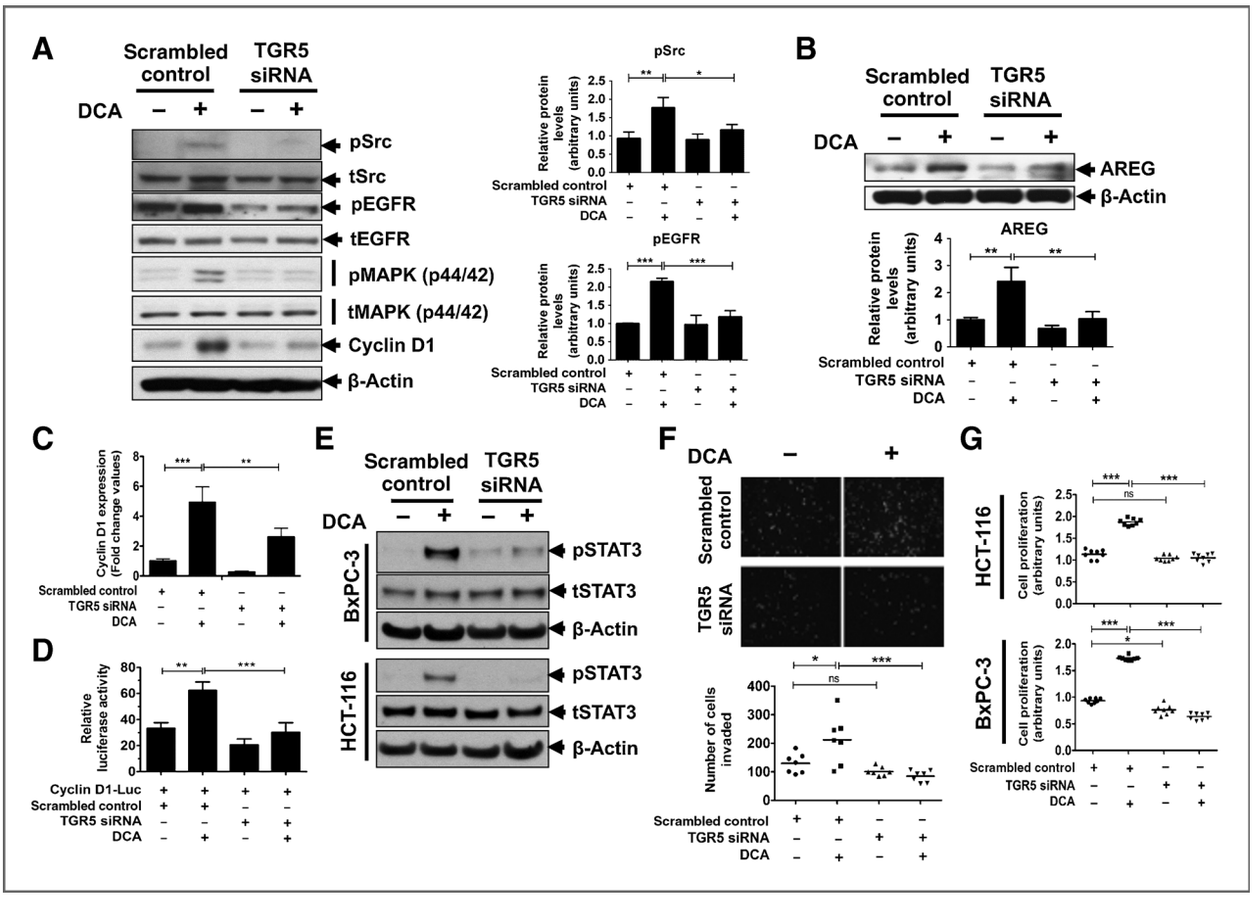

Figure 6. TGR5 is responsible for DCA-induced activation of Src, EGFR, and STAT3 signaling. A, DCA-treated (300 μmol/L) TGR5 knockdown BxPC-3 cells show a significant reduction in the phosphorylation of Src, EGFR, and MAPK and inhibition of DCA-induced expression of cyclin D1 (left). Quantitative analysis from three independent immunoblots of Src and EGFR phosphorylation normalized to total Src and EGFR expression levels, respectively (right). B, BxPC-3 cells from scrambled control and TGR5 siRNA were investigated for DCA-induced AREG protein expression (top). Quantitative analysis from three independent immunoblots of AREG was normalized to β-actin expression levels (bottom). C, quantitative real-time PCR of TGR5 knockdown BxPC-3 cells show significantly decreased transcription of the cyclin D1 gene compared with scrambled control cells. D, the luciferase assay using the cyclin D1 reporter shows induction of cyclin D1 transcriptional activity with DCA exposure in scrambled control BxPC-3 cells, which is inhibited in TGR5 siRNA cells. E, DCA (10 μmol/L) exposure to TGR5 knockdown BxPC3 and HCT-116 cells shows a significant reduction in the phosphorylation of STAT3. F and G, DCA (300 μmol/L) exposure to TGR5 knockdown cells shows a significant reduction in the cell invasion (F) and cell proliferation (G) when compared with scrambled control cells treated with DCA alone. Individual data point, mean ± SD ($n = 3$) for A–D or mean ± SD for F ($n = 7$) and G ($n = 8$). (*, $P < 0.05$; **, $P < 0.01$; ***, $P < 0.001$; ns, nonsignificant).

Cyclin D1 is a transcription target of the MAPK that plays an important role in cell proliferation, tumor development, and progression (45). Our data show that DCA exposure significantly increases expression and promoter activity of cyclin D1, which is TGR5 receptor mediated, whereas knockdown of AREG or TGR5 significantly reduced these effects. Consistent with this result, the rate of DNA synthesis and cell proliferation induced by DCA treatment was significantly reduced by the siRNA-based knockdown of Src and AREG in colorectal cancer and PDAC cells. EGFR activation induces STAT3 signaling (10). Our results describe that DCA induces EGFR–STAT3 signaling, which plays an important role in cancer progression. DCA works through TGR5–Src–TACE–AREG–EGFR activation, which then leads to activation of EGFR downstream pathways, such as MAPK–cyclin D1 and STAT3, to promote cancer growth and indicates that AREG is an important molecular target of growth-promoting actions of DCA. Collectively, these results on DCA-induced stimulation of the AREG-ligand regulated pathways in colorectal cancer and PDAC provide further insight into the molecular events of tumor promotion by secondary BAs. The data reported in this study summarized schematically in Supplementary Fig. S9.

In summary, this study provides the first evidence, to our knowledge, that DCA can stimulate the association of Src and TACE through the G protein-coupled BA receptor TGR5 and has identified AREG as a critical EGFR ligand in DCA-dependent tumorigenicity. Aberrant enhancement of EGFR ligand expression is speculated to be one of several different molecular mechanisms, including receptor mutations, constitutive activation of downstream pathways, and activation of alternative pathways, for the acquired resistance against EGFR antagonists (46). Thus, a particular EGFR ligand that is

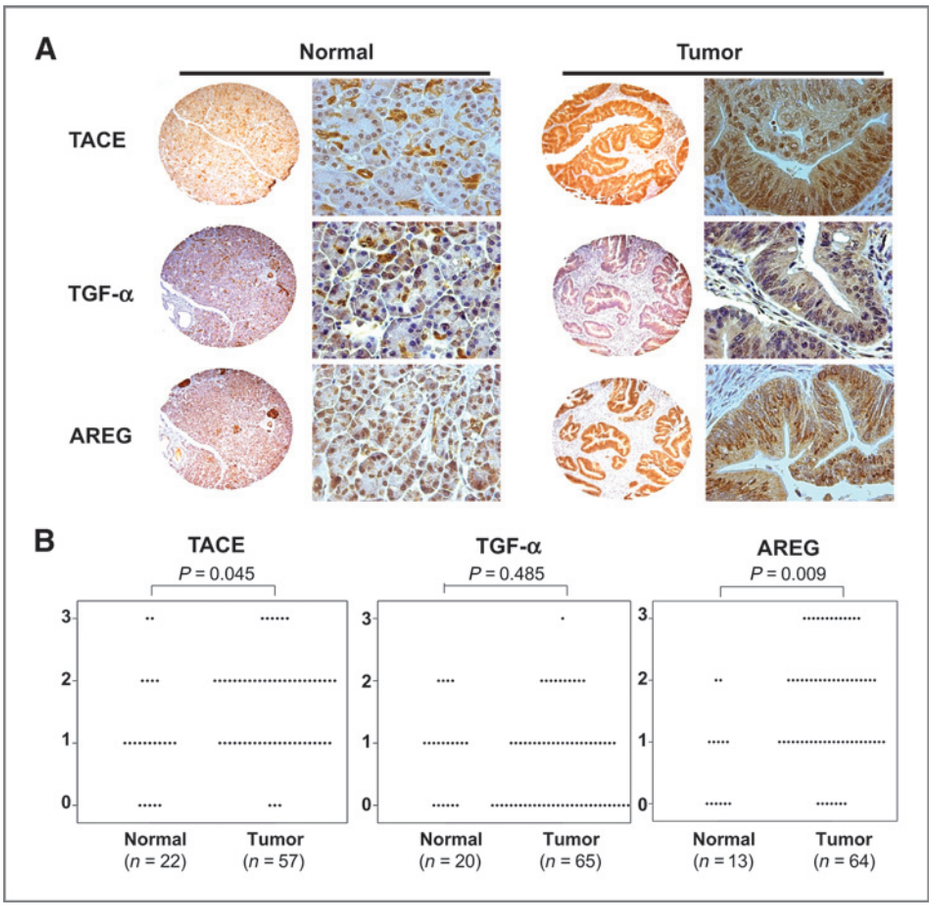

Figure 7. Distribution of differences in TACE, TGF-α, and AREG staining between normal human pancreas tissue and pancreatic tumors. A, distribution of the difference in intensity staining between normal ducts and tumors for TACE, TGF-α, and AREG is shown. Expression of these proteins was scored as 0 to 3+ in intensity and the percentage of positive tumor cells was estimated. B, diamond plots show the distribution of differences in TACE, TGF-α, and AREG staining in tumors compared with normal pancreatic tissue. Differences >0 describe tumor tissue with higher levels of protein staining than normal pancreas, whereas differences <0 describe levels of protein staining greater in normal pancreas.

predominantly expressed in human cancer can be recognized as an attractive target itself. Patients with metastatic lung, colorectal, pancreatic, or head and neck cancers who initially benefit from EGFR-targeted therapies eventually developed resistance (47). Previous studies have suggested that inhibiting AREG activity may be necessary to overcome the resistance to EGFR-targeted therapies in non–small cell lung cancer (NSCLC; ref. 48) and hepatocellular carcinoma (49). This is consistent with recent reports showing that inhibiting AREG activity is associated with a better response to cetuximab in colorectal cancer and that AREG overexpression in patients with NSCLC correlates with a poor response to gefitinib (38, 50). This novel finding may lead to the validation of Src and TACE association–induced AREG activity as a clinically valuable cancer biomarker, which can be used to discriminate sensitive from resistant tumors, and provides increased therapeutic options to treat EGFR-resistant colorectal cancer and PDAC tumors.

Disclosure of Potential Conflicts of Interest

No potential conflicts of interest were disclosed.

Authors' Contributions

Conception and design: N.S. Nagathihalli, W. Lee, A.C. Lockhart, N.B. Merchant
Development of methodology: N.S. Nagathihalli, M.K. Washington, N.B. Merchant
Acquisition of data (provided animals, acquired and managed patients, provided facilities, etc.): N.S. Nagathihalli, Y. Beesetty, W. Lee, N.B. Merchant
Analysis and interpretation of data (e.g., statistical analysis, biostatistics, computational analysis): N.S. Nagathihalli, M.K. Washington, X. Chen, N.B. Merchant
Writing, review, and/or revision of the manuscript: N.S. Nagathihalli, W. Lee, M.K. Washington, A.C. Lockhart, N.B. Merchant
Administrative, technical, or material support (i.e., reporting or organizing data, constructing databases): N.S. Nagathihalli, Y. Beesetty, N.B. Merchant
Study supervision: N.S. Nagathihalli, N.B. Merchant

Acknowledgments

The authors thank Dr. Igor Voskresensky for assistance with sample preparation for radioimmunoassay analysis, Bakula Trivedi for assistance with the radioimmunoassay analysis and Frank Revetta for his technical assistance with immunohistochemical staining, and Jay Gibbons from Wyeth-Aherst (Pearl River, NY) for providing WAY-022.

Grant Support

This work was supported by the NIH grants CA161976, P50 95103 GI Special Program of Research Excellence Grant (SPORE), 5P30DK058404-08 Vanderbilt Digestive Disease Research Center (DDRC) Translational Award, and Vanderbilt-Ingram Cancer Center Support grant 5P30 CA068485-1. Core services were performed through the NIH DDRC P30DK058404 grant (N.B. Merchant and N.S. Nagathihalli).

The costs of publication of this article were defrayed in part by the payment of page charges. This article must therefore be hereby marked *advertisement* in accordance with 18 U.S.C. Section 1734 solely to indicate this fact.

Received August 13, 2013; revised January 3, 2014; accepted January 31, 2014; published OnlineFirst February 11, 2014.

References

1. Bayerdorffer E, Mannes GA, Richter WO, Ochsenkuhn T, Wiebecke B, Kopcke W, et al. Increased serum deoxycholic acid levels in men with colorectal adenomas. Gastroenterology 1993;104:145–51.
2. Debruyne PR, Bruyneel EA, Li X, Zimber A, Gespach C, Mareel MM. The role of bile acids in carcinogenesis. Mutat Res 2001;480–481: 359–69.
3. Bernstein H, Bernstein C, Payne CM, Dvorak K. Bile acids as endogenous etiologic agents in gastrointestinal cancer. World J Gastroenterol 2009;15:3329–40.
4. Jenkins GJ, Harries K, Doak SH, Wilmes A, Griffiths AP, Baxter JN, et al. The bile acid deoxycholic acid (DCA) at neutral pH activates NF-kappaB and induces IL-8 expression in oesophageal cells *in vitro*. Carcinogenesis 2004;25:317–23.
5. Tselepis C, Morris CD, Wakelin D, Hardy R, Perry I, Luong QT, et al. Upregulation of the oncogene c-myc in Barrett's adenocarcinoma: induction of c-myc by acidified bile acid *in vitro*. Gut 2003;52:174–80.
6. Yoshimoto S, Loo TM, Atarashi K, Kanda H, Sato S, Oyadomari S, et al. Obesity-induced gut microbial metabolite promotes liver cancer through senescence secretome. Nature 2013;499:97–101.
7. Bernstein C, Bernstein H, Payne CM, Dvorak K, Garewal H. Field defects in progression to gastrointestinal tract cancers. Cancer Lett 2008;260:1–10.
8. Daub H, Weiss FU, Wallasch C, Ullrich A. Role of transactivation of the EGF receptor in signalling by G-protein-coupled receptors. Nature 1996;379:557–60.
9. Carpenter G. Employment of the epidermal growth factor receptor in growth factor-independent signaling pathways. J Cell Biol 1999;146:697–702.
10. Grandis JR, Drenning SD, Chakraborty A, Zhou MY, Zeng Q, Pitt AS, et al. Requirement of Stat3 but not Stat1 activation for epidermal growth factor receptor–mediated cell growth *in vitro*. J Clin Invest 1998;102:1385–92.
11. Kawamata Y, Fujii R, Hosoya M, Harada M, Yoshida H, Miwa M, et al. A G protein-coupled receptor responsive to bile acids. J Biol Chem 2003;278:9435–40.
12. Merchant NB, Rogers CM, Trivedi B, Morrow J, Coffey RJ. Ligand-dependent activation of the epidermal growth factor receptor by secondary bile acids in polarizing colon cancer cells. Surgery 2005;138:415–21.
13. Merchant NB, Voskresensky I, Rogers CM, Lafleur B, Dempsey PJ, Graves-Deal R, et al. TACE/ADAM-17: a component of the epidermal growth factor receptor axis and a promising therapeutic target in colorectal cancer. Clin Cancer Res 2008;14:1182–91.
14. Lee DC, Sunnarborg SW, Hinkle CL, Myers TJ, Stevenson MY, Russell WE, et al. TACE/ADAM17 processing of EGFR ligands indicates a role as a physiological convertase. Ann N Y Acad Sci 2003;995:22–38.
15. Kenny PA, Bissell MJ. Targeting TACE-dependent EGFR ligand shedding in breast cancer. J Clin Invest 2007;117:337–45.
16. Harris RC, Chung E, Coffey RJ. EGF receptor ligands. Exp Cell Res 2003;284:2–13.
17. Gschwind A, Hart S, Fischer OM, Ullrich A. TACE cleavage of proamphiregulin regulates GPCR-induced proliferation and motility of cancer cells. EMBO J 2003;22:2411–21.
18. Zhang Q, Thomas SM, Lui VW, Xi S, Siegfried JM, Fan H, et al. Phosphorylation of TNF-alpha converting enzyme by gastrin-releasing peptide induces amphiregulin release and EGF receptor activation. Proc Natl Acad Sci U S A 2006;103:6901–6.
19. Irby RB, Yeatman TJ. Increased Src activity disrupts cadherin/catenin-mediated homotypic adhesion in human colon cancer and transformed rodent cells. Cancer Res 2002;62:2669–74.
20. Nagaraj NS, Smith JJ, Revetta F, Washington MK, Merchant NB. Targeted inhibition of SRC kinase signaling attenuates pancreatic tumorigenesis. Mol Cancer Ther 2010;9:2322–32.
21. Allgayer H, Boyd DD, Heiss MM, Abdalla EK, Curley SA, Gallick GE. Activation of Src kinase in primary colorectal carcinoma—an indicator of poor clinical prognosis. Cancer 2002;94:344–51.
22. Chang YM, Bai L, Liu S, Yang JC, Kung HJ, Evans CP. Src family kinase oncogenic potential and pathways in prostate cancer as revealed by AZD0530. Oncogene 2008;27:6365–75.
23. Serrels B, Serrels A, Mason SM, Baldeschi C, Ashton GH, Canel M, et al. A novel Src kinase inhibitor reduces tumour formation in a skin carcinogenesis model. Carcinogenesis 2009;30:249–57.
24. Maretzky T, Zhou W, Huang XY, Blobel CP. A transforming Src mutant increases the bioavailability of EGFR ligands via stimulation of the cell-surface metalloproteinase ADAM17. Oncogene 2011;30: 611–8.
25. Van Schaeybroeck S, Kelly DM, Kyula J, Stokesberry S, Fennell DA, Johnston PG, et al. Src and ADAM-17-mediated shedding of transforming growth factor-alpha is a mechanism of acute resistance to TRAIL. Cancer Res 2008;68:8312–21.
26. Cates JM, Byrd RH, Fohn LE, Tatsas AD, Washington MK, Black CC. Epithelial–mesenchymal transition markers in pancreatic ductal adenocarcinoma. Pancreas 2009;38:e1–6.
27. Scheiman JM, Meise KS, Greenson JK, Coffey RJ. Transforming growth factor-alpha (TGF-alpha) levels in human proximal gastrointestinal epithelium. Effect of mucosal injury and acid inhibition. Dig Dis Sci 1997;42:333–41.
28. Nagaraj NS, Beckers S, Mensah JK, Waigel S, Vigneswaran N, Zacharias W. Cigarette smoke condensate induces cytochromes P450 and aldo-keto reductases in oral cancer cells. Toxicol Lett 2006;165: 182–94.
29. Tetsu O, McCormick F. Beta-catenin regulates expression of cyclin D1 in colon carcinoma cells. Nature 1999;398:422–6.
30. Nagaraj NS, Vigneswaran N, Zacharias W. Hypoxia inhibits TRAIL-induced tumor cell apoptosis: involvement of lysosomal cathepsins. Apoptosis 2007;12:125–39.
31. Nagaraj NS, Washington MK, Merchant NB. Combined blockade of Src kinase and epidermal growth factor receptor with gemcitabine overcomes STAT3-mediated resistance of inhibition of pancreatic tumor growth. Clin Cancer Res 2011;17:483–93.
32. Pols TW, Noriega LG, Nomura M, Auwerx J, Schoonjans K. The bile acid membrane receptor TGR5 as an emerging target in metabolism and inflammation. J Hepatol 2011;54:1263–72.
33. Hong J, Behar J, Wands J, Resnick M, Wang LJ, DeLellis RA, et al. Role of a novel bile acid receptor TGR5 in the development of oesophageal adenocarcinoma. Gut 2010;59:170–80.
34. Santiskulvong C, Sinnett-Smith J, Rozengurt E. EGF receptor function is required in late G(1) for cell cycle progression induced by bombesin and bradykinin. Am J Physiol Cell Physiol 2001;281: C886–98.
35. Qiao D, Stratagouleas ED, Martinez JD. Activation and role of mitogen-activated protein kinases in deoxycholic acid-induced apoptosis. Carcinogenesis 2001;22:35–41.
36. Yoon JH, Higuchi H, Werneburg NW, Kaufmann SH, Gores GJ. Bile acids induce cyclooxygenase-2 expression via the epidermal growth factor receptor in a human cholangiocarcinoma cell line. Gastroenterology 2002;122:985–93.
37. Baselga J, Arteaga CL. Critical update and emerging trends in epidermal growth factor receptor targeting in cancer. J Clin Oncol 2005;23:2445–59.
38. Ishikawa N, Daigo Y, Takano A, Taniwaki M, Kato T, Hayama S, et al. Increases of amphiregulin and transforming growth factor-alpha in serum as predictors of poor response to gefitinib among patients with advanced non–small cell lung cancers. Cancer Res 2005;65: 9176–84.
39. Blobel CP. ADAMs: key components in EGFR signalling and development. Nat Rev Mol Cell Biol 2005;6:32–43.
40. Castillo J, Erroba E, Perugorria MJ, Santamaria M, Lee DC, Prieto J, et al. Amphiregulin contributes to the transformed phenotype of human hepatocellular carcinoma cells. Cancer Res 2006;66:6129–38.
41. Cook PW, Pittelkow MR, Keeble WW, Graves-Deal R, Coffey RJ Jr, Shipley GD. Amphiregulin messenger RNA is elevated in psoriatic epidermis and gastrointestinal carcinomas. Cancer Res 1992;52: 3224–7.
42. Saeki T, Stromberg K, Qi CF, Gullick WJ, Tahara E, Normanno N, et al. Differential immunohistochemical detection of amphiregulin and cripto in human normal colon and colorectal tumors. Cancer Res 1992; 52:3467–73.

43. Nicholson RI, Gee JM, Harper ME. EGFR and cancer prognosis. Eur J Cancer 2001;37:S9–15.
44. Fang JY, Richardson BC. The MAPK signalling pathways and colorectal cancer. Lancet Oncol 2005;6:322–7.
45. Dhillon AS, Hagan S, Rath O, Kolch W. MAP kinase signalling pathways in cancer. Oncogene 2007;26:3279–90.
46. Morgillo F, Lee HY. Resistance to epidermal growth factor receptor-targeted therapy. Drug Resist Updat 2005;8:298–310.
47. Chong CR, Janne PA. The quest to overcome resistance to EGFR-targeted therapies in cancer. Nat Med 2013;19:1389–400.
48. Busser B, Sancey L, Josserand V, Niang C, Favrot MC, Coll JL, et al. Amphiregulin promotes BAX inhibition and resistance to gefitinib in non–small cell lung cancers. Mol Ther 2010;18:528–35.
49. Hopfner M, Sutter AP, Huether A, Schuppan D, Zeitz M, Scherubl H. Targeting the epidermal growth factor receptor by gefitinib for treatment of hepatocellular carcinoma. J Hepatol 2004;41:1008–16.
50. Baker JB, Dutta D, Watson D, Maddala T, Munneke BM, Shak S, et al. Tumour gene expression predicts response to cetuximab in patients with KRAS wild-type metastatic colorectal cancer. Br J Cancer 2011;104:488–95.